Molecular Biology of the Cell
Vol. 20, 2979–2990, June 15, 2009

Normal Formation of a Subset of Intestinal Granules in *Caenorhabditis elegans* Requires ATP-binding Cassette Transporters HAF-4 and HAF-9, Which Are Highly Homologous to Human Lysosomal Peptide Transporter TAP-Like

Hiromi Kawai,*† Takahiro Tanji,†‡ Hirohisa Shiraishi,†‡ Mitsuo Yamada,* Ryoko Iijima,* Takao Inoue,§ Yasuko Kezuka,* Kazuaki Ohashi,* Yasuo Yoshida,‖ Koujiro Tohyama,‖ Keiko Gengyo-Ando,¶ Shohei Mitani,¶ Hiroyuki Arai,§ Ayako Ohashi-Kobayashi,*‡ and Masatomo Maeda*#

*Department of Molecular Biology and Biochemistry, Graduate School of Pharmaceutical Sciences, Osaka University, Suita, Osaka 565-0871, Japan; ‡Department of Immunobiology, School of Pharmacy, Iwate Medical University, Yahaba, Shiwa-gun, Iwate 028-3694, Japan; §Department of Health Chemistry, Graduate School of Pharmaceutical Sciences, The University of Tokyo, Bunkyo-ku, Tokyo 113-0033, Japan; ‖The Center for Electron Microscopy and Bio-Imaging Research, Iwate Medical University, Morioka, Iwate 020-8505, Japan; and ¶Department of Physiology, School of Medicine, Tokyo Women's Medical University, Shinjuku-ku, Tokyo 162-8666, Japan

Submitted September 8, 2008; Revised April 10, 2009; Accepted April 17, 2009
Monitoring Editor: Thomas F.J. Martin

TAP-like (TAPL; ABCB9) is a half-type ATP-binding cassette (ABC) transporter that localizes in lysosome and putatively conveys peptides from cytosol to lysosome. However, the physiological role of this transporter remains to be elucidated. Comparison of genome databases reveals that TAPL is conserved in various species from a simple model organism, *Caenorhabditis elegans*, to mammals. *C. elegans* possesses homologous TAPL genes: *haf-4* and *haf-9*. In this study, we examined the tissue-specific expression of these two genes and analyzed the phenotypes of the loss-of-function mutants for *haf-4* and *haf-9* to elucidate the in vivo function of these genes. Both HAF-4 and HAF-9 tagged with green fluorescent protein (GFP) were mainly localized on the membrane of nonacidic but lysosome-associated membrane protein homologue (LMP-1)-positive intestinal granules from larval to adult stage. The mutants for *haf-4* and *haf-9* exhibited granular defects in late larval and young adult intestinal cells, associated with decreased brood size, prolonged defecation cycle, and slow growth. The intestinal granular phenotype was rescued by the overexpression of the GFP-tagged wild-type protein, but not by the ATP-unbound form of HAF-4. These results demonstrate that two ABC transporters, HAF-4 and HAF-9, are related to intestinal granular formation and some other physiological aspects.

INTRODUCTION

ATP-binding cassette (ABC) transporters form the largest superfamily among the various kinds of transporter families (Higgins, 1992; Dean and Annilo, 2005); however, many of their functions remain to be elucidated. Especially, substrates and subcellular localization of half-type ABC transporters have been less investigated, with the exception of transporter associated with antigen processing (TAP) and a few mitochondrial transporters (Kleijmeer *et al*., 1992; Uebel *et al*., 1997; Young *et al*., 2001).

TAP-like (TAPL; ABCB9) is a mammalian half-type ABC transporter that is highly homologous to TAP1 (ABCB2) and TAP2 (ABCB3), each of which is a subunit of heterodimeric peptide transporter TAP (Yamaguchi *et al*., 1999; Zhang *et al*., 2000; Kobayashi *et al*., 2000). From its sequence similarity with TAP1 and TAP2, TAPL is inferred to transport peptides as substrates; indeed, it transports various sizes of peptides in vitro (Wolters *et al*., 2005; Zhao *et al*., 2008). Localization of TAPL to lysosome was observed in an overexpression study of mammalian culture cells and also by immunohistochemistry in lysosome-rich Sertoli cells, monocyte-derived cells in testis (Zhang *et al*., 2000). The difference in the tissue-specific expression between mammalian TAPL and TAP1/TAP2 suggests that TAPL has its own role, which differs from major histocompatibility complex (MHC) class I-restricted

This article was published online ahead of print in *MBC in Press* (http://www.molbiolcell.org/cgi/doi/10.1091/mbc.E08–09–0912) on April 29, 2009.

† These authors contributed equally to this work.

Present address: Department of Molecular Biology, School of Pharmacy, Iwate Medical University, 2-1-1 Nishitokuta, Yahaba, Shiwa-gun, Iwate 028-3694, Japan.

Address correspondence to: Ayako Ohashi-Kobayashi (aohashi@iwate-med.ac.jp).

Abbreviations used: ABC, ATP-binding cassette; DIC, differential interference contrast; DMSO, dimethyl sulfoxide; GFP, green fluorescent protein; LAMP, lysosome-associated membrane protein; mRFP, monomeric red fluorescent protein; MRP, multidrug resistance-associated protein; PBS, phosphate-buffered saline; PBS-T, PBS containing 0.1%, wt/wt, Tween-20; TAP, transporter associated with antigen processing; TAPL, TAP-like.

antigen transporter TAP (Kobayashi *et al*., 2003; Yamaguchi *et al*., 2004). Recent reports describe that overexpression of TAPL did not restore MHC class I surface expression in TAP-deficient cells, although TAPL expression is strongly induced during differentiation of monocytes to dendritic cells or macrophages (Demirel *et al*., 2007). Furthermore, the strong conservation of genomic structure among three genes, TAP1, TAP2, and TAPL (Kobayashi *et al*., 2003), along with the finding of invertebrate homologues of TAPL in fly and nematode, suggests that TAPL is an ancestral gene of TAP preceding the advent of acquired immunity.

To investigate the in vivo function of TAPL, we specifically examined a model organism, the nematode *Caenorhabditis elegans*, for which genetic and molecular biological methods have been established. *C. elegans* possesses 60 ABC transporter genes, including some with only partial sequences (Sheps *et al*., 2004). These ABC transporter genes are now categorized as subfamilies A to G according to the mammalian ABC transporter subfamily classification. For example, *ced-7*, identified as a cell corpse engulfment gene in *C. elegans*, encodes a member of the ABC transporter A subfamily, members of which are strongly connected to lipid transport (Wu and Horvitz, 1998). Other examples are multidrug resistance-associated protein (MRP)-1 and MRP-4, which are regulators of dauer diapause and key proteins of lysosomal function in coelomocyte and embryo (Yabe *et al*., 2005; Schaheen *et al*., 2006; Currie *et al*., 2007). They are members of the ABC transporter D subfamily, which is known as the MRP group involved in anionic substance transport.

Among *C. elegans* ABC transporter genes, 19 full-type and nine half-type B subfamily members have been identified. That is, almost half of the ABC transporter genes in *C. elegans* belong to the B subfamily, which is also known as the TAP/multidrug resistance (MDR) group, although the largest subfamily of mammalian ABC transporter is A (Dean and Annilo, 2005). Some members of the B subfamily in *C. elegans* are characterized according to their drug and heavy metal resistance (Broeks *et al*., 1996; Lindblom *et al*., 2001; Vatamaniuk *et al*., 2005), innate immunity (Mahajan-Miklos *et al*., 1999; Kurz *et al*., 2007), fat storage (Nunes *et al*., 2005; Schroeder *et al*., 2007), and RNA interference mechanism (Sundaram *et al*., 2006). In this report, we analyzed two *C. elegans* TAPL homologues, HAF-4 and HAF-9, which have the highest sequence identity with human TAPL. The phenotypes of mutants that were defective in the TAPL homologues were investigated along with their tissue distribution and subcellular localization.

MATERIALS AND METHODS

General Methods and Mutant Strains

Maintenance, husbandry, and genetic crosses of *C. elegans* were performed according to standard protocols by Brenner (1974). Strains were cultured at 20°C unless otherwise mentioned. The Bristol strain N2 was used as the standard wild-type strain. The following mutant strains were obtained from *Caenorhabditis* Genetics Center (University of Minnesota, Minneapolis, MN): *haf-1(ok705)*, *haf-2(gk13)*, *haf-3(ok1086)*, *haf-4(ok1042)*, *haf-4(gk240)*, *haf-5(gk155)*, *haf-5(gk161)*, *haf-7(gk46)*, *haf-8(gk12)*, *haf-9(gk23)*, *lmp-1(nr2045)*, *ppk-3(n2668)*, and *rab-10(q373)*. *ppk-3(n2668)* was provided by Dr. J. Laporte (Université Louis Pasteur de Strasbourg, Illkirch, France) (Nicot *et al*., 2006).

Transgenic Strains

Genome cloning of *haf-4 I* and *haf-9 I* was performed by polymerase chain reaction (PCR) using genome isolated from an adult of N2 as a template. Their sequences were confirmed by comparison with assigned sequences on the National Center for Biotechnology Information (NCBI) database (*C. elegans* Sequencing Consortium, 1998).

Transgenic strains were all generated for this study except *Is*[*hsp-60::mRFP*] which was provided by Dr. T. Oka (Kyushu University, Fukuoka, Japan). To generate *haf-4::GFP* construct, SphI-SpeI *haf-4* genome clone containing the promoter region (2086 base pairs region upstream of the initiation codon) was inserted into the pPD95.77 vector with SphI and XbaI sites. *haf-9::GFP* construct was created by inserting SphI-BamHI *haf-9* genome clone with 2739 base pairs of the upstream sequence into the pPD95.75 vector. To generate the lysosomal markers, the pFX series of vectors that the green fluorescent protein (GFP) or red fluorescent protein (RFP) would be fused to the C terminus of the proteins (Gengyo-Ando *et al*., 2006) were used. The *ges-1* promoter (3.3 kb) and the *lmp-1* cDNA containing the complete coding sequence (711 base pairs) were inserted into the pFXneEGFP, and then the enhanced (E)GFP sequence was replaced by the monomeric RFP sequence (*Pges-1::lmp-1::mRFP*).

For introduction of the Walker A mutation (K539M) in the *haf-4* construct, site-directed mutagenesis was performed using PCR with Pyrobest DNA polymerase (Takara Bio, Ohtsu, Japan) (Imai *et al*., 1991) and *haf-4::GFP* construct as a template. The following primers were used for PCR: forward primer, 5′-TGGCTCTGGAATGTCTCGTGCATTTC-3′; and reverse primer, 5′-GCACGAAGACATTCCAGAGGCAGATG-3′.

Microinjection of DNA into the *C. elegans* germline was carried out as described by Mello *et al*. (1991) using pRF4 [*rol-6(su1006)*] as a selection marker. Integrant formation of *haf-4::GFP*, *haf-9::GFP*, *haf-4(K539M)::GFP*, and *Pges-1::lmp-1::mRFP* transgenic worms was performed according to Mitani's method (Mitani, 1995).

Optical Microscopic Observation

The differential interference contrast (DIC) and polarization images were analyzed using microscopy (IX70, BX51; Olympus, Tokyo, Japan) with DIC and polarization optics. Fluorescence images were analyzed using the 488-nm excitation line of an argon laser and WIG/WIY filter units. Confocal fluorescence images were obtained using a confocal microscope (FV-1000; Olympus) with 473- or 559-nm excitation lines of light-emitting diode lasers. Spectral scanning and unmixing were performed with a spectral deconvolution program of FV-1000 software FV10-ASW (Olympus).

All pictures were taken using hermaphrodites at day-1 adult stage except *Is*[*Pges-1::lmp-1::mRFP*], although larval stage (L)4 worms showed identical results. For *Is*[*Pges-1::lmp-1::mRFP*], pictures at the L4 stage are presented because overexpression of LMP-1::monomeric red fluorescent protein (mRFP) disrupted intestinal granular formation at the adult stage. All pictures presented are oriented with the anterior to the left. For granular counts, the number of granules with a diameter of 1 μm or more was counted manually per 300 μm^2 on the DIC image for each worm.

Antisera Preparation

For anti-HAF-4 and anti-HAF-9 sera preparation, the cDNA fragment for the ABC region was inserted into pET28a (Merck Chemicals; Nottingham, United Kingdom). The recombinant protein tagged with 6×His was expressed by BL21(DE3) (Agilent Technologies, Santa Clara, CA) and purified with TALON Metal Affinity Resin (Takara Bio). Rabbit anti-HAF-4 and HAF-9 sera were obtained 6 and 8 wk, respectively, after the inoculation of the purified protein. The specificity of the antisera was tested using the *haf-4(ok1042)*, *haf-4(gk240)*, and *haf-9(gk23)* deletion mutants.

Membrane Fractionation and Western Blot

Adult worms were put on two 9-cm NG agar plates (Brenner, 1974) for each strain (~15 worms/plate) seeded with *Escherichia coli* (OP50) and reared for 2 d. Mixed stage worms were harvested from the two plates into a 15-ml conical tube with 5 ml of M9 buffer (Brenner, 1974) containing 20 mM NaN_3. After centrifuging at 1000 × *g* for 5 min at 20°C (T4SS31 rotor, CF16RXII centrifuge; Hitachi, Tokyo, Japan), the worms were transferred into a 2-ml centrifuge tube with 1 ml of M9 buffer and then washed with 1 ml of M9 buffer three times. The collected worms were frozen with liquid nitrogen and stored at −80°C.

The frozen worms were suspended in 2 volumes (200–300 μl) of 50 mM Tris-HCl, pH 7.5, containing 250 mM sucrose, 25 mM potassium acetate, 5 mM magnesium acetate, and protease inhibitor cocktail (Complete, Mini, EDTA-free; Roche Diagnostics, Tokyo, Japan), sonicated for 20 s × 8 with 1-min interval on ice by using a homogenizer (output level 7, Ultra S Homogenizer VP-5S; Taitec, Koshigaya, Japan), and then fractionated by centrifugation at 1500 × *g* for 15 min (T11A32 rotor, CF16RXII centrifuge) followed by ultracentrifugation at 33,000 rpm for 1 h at 4°C (TLA-100.4 rotor; 1.5-ml microfuge tube [357448] with adaptor [360951]; Optima TL ultracentrifuge; Beckman Coulter, Fullerton, CA). The resulting supernatant was collected as a soluble fraction. The precipitate was suspended in 200 μl of 20 mM HEPES-NaOH, pH 7.5, containing 25% glycerol and protease inhibitor cocktail, incubated at 4°C for 16 h, and then the supernatant was collected as an insoluble membrane fraction after centrifuging at 1500 × *g* for 10 min (T11A32 rotor, CF16RXII centrifuge).

The fractionated samples (10 μg protein/lane) were treated at 55°C for 10 min and then separated by SDS-polyacrylamide gel electrophoresis (PAGE) (20 mA, 80 min; e-PAGEL 5–20%; Atto, Tokyo, Japan) and electroblotted (200 mA, 2 h; model AE6677; Atto) onto an Immobilon transfer membrane

(Millipore, Billerica, MA) that was subsequently incubated at 4°C for 16 h in blocking solution (5%, wt/vol, nonfat dry milk [Hokkaido Nyugyou, Hakodate, Japan] in phosphate-buffered saline [PBS]). The blot was probed with anti-HAF-4 or anti-HAF-9 serum (5000× dilution with PBS-0.1%, wt/wt, Tween 20 [PBS-T]), followed by the reaction with a goat anti-rabbit horseradish-peroxidase-conjugated antibody (Thermo Fisher Scientific, Waltham, MA) (4000× dilution with PBS-T). Alternatively, anti-GFP peroxidase-conjugated (Nacalai Tesque, Kyoto, Japan) (1000× dilution with PBS-T) was used for the HAF-4::GFP and HAF-9::GFP detection. Target protein detection was performed using SuperSignal West Femto Maximum Sensitivity Substrate (Thermo Fisher Scientific) and the image analyzer LAS-3000 (Fujifilm, Tokyo, Japan).

Subcellular Compartment Labeling with Dyes

Acidic compartments were stained with acridine orange (Sigma-Aldrich, St. Louis, MO) or LysoTracker Red DND-99 (Invitrogen, Carlsbad, CA). For acridine orange staining, 100 μl of 0.01 mg/ml acridine orange in M9 buffer was spread onto the entire surface of an NG agar plate (3.5 cm in diameter) seeded with OP50. After the dye solution was dried up, 1-d young adult worms were kept on the plate for 2 h and then observed under a confocal microscope. For LysoTracker Red staining, 5 μl of 1 mM LysoTracker Red DND-99 in dimethyl sulfoxide (DMSO) was dropped onto an OP50 lawn on an NG agar plate. Late larval worms were reared on the plate for 1 d, and then young adult worms were observed under an epifluorescence microscope.

For the staining of lipophilic compartments, 5 μl of 0.1 mM Nile Red (Sigma-Aldrich) in DMSO was dropped onto an OP50 lawn on an NG agar plate. L1 or L2 starved larvae were transferred onto the plate and reared for 1 d at 25°C, and then young adult worms were observed under an epifluorescence microscope.

Electron Microscopic Observation

Worms were processed for transmission electron microscopy of ultrathin sections as follows. Briefly, young adult worms were anesthetized in 50 mM NaN_3 in M9 buffer for 5 min and then collected in a 2-ml microtube. After rinsing the worms with M9 buffer once, they were fixed for 16 h with gentle rotation in 2.5% glutaraldehyde and 1% paraformaldehyde in 0.05 M sodium cacodylate-HCl, pH 7.3, 0.1 M sucrose, 0.1 mM $MgCl_2$ at 4°C. The worms were rinsed with ice-chilled 0.2 M cacodylate buffer, pH 7.3, three times and postfixed for 2 h in 1% osmium tetroxide in 0.1 M cacodylate buffer at 4°C. After washing the worms with 0.1 M cacodylate buffer twice, dehydration in graded ethanol:water mixes (50%, 75%, and 95% once for 10 min, respectively, and 100% three times for 10 min per change) was performed. For use in this study, 100% ethanol was prepared by treating absolute ethanol (99.5%) with copper sulfate anhydride.

Infiltration of resin was carried out as follows. The dehydrated worms were treated with the mixture of equivalent volumes of ethanol and *n*-butyl glycidyl ether (QY-1) (Nisshin EM, Tokyo, Japan) for 30 min and then immersed in QY-1 alone twice for 30 min each. They were treated sequentially with 1 part resin (Plain Resin; Nisshin EM) to 2 parts QY-1 for 3 h, 2 parts resin to 1 part resin for 16 h, and resin alone three times for 3 h per change. After embedding the samples in fresh resin in a silicon mold, the resin was polymerized for 1 d at 50°C followed by an additional 3 d of incubation at 65°C. Ultrathin sections were cut to a thickness of ~90 nm by using an ultramicrotome (Ultracut-UCT; Leica Microsystems, Wetzlar, Germany) and mounted on copper grids. The sections were counterstained with 1% uranyl acetate for 30 min, followed by Reynold's lead citrate staining for 5 min; then, they were observed using a transmission electron microscope (H-7650; Hitachi).

Growth Rate Measurement and Other Assays

For brood size measurement, a single L4 hermaphrodite was reared on an NG agar plate with the plate being changed everyday until the worm stopped laying fertilized eggs. Hatched larvae from each parent were summated as the brood size. Ten worms for each strain were subjected to the analysis. Parental worms were censored if they crawled off the media.

For growth rate measurement, five to 10 gravid adult hermaphrodites were transferred to new agar media (6 cm in diameter). Eggs were laid for 3 h, and then adults were removed. The quantities of F_1 adults were counted every 3 h. Pharyngeal pumping assay (Raizen *et al*., 1995) and defecation rhythm assay (Thomas, 1990) were performed according to methods described respectively in original reports.

Other Chemicals

Restriction enzymes and modifying enzymes were purchased from New England Biolabs (Ipswich, MA), Takara Bio, and Promega (Madison, WI). The PCR primers were purchased from Gene Design (Ibaraki, Japan). DNA sequence determination was performed using a sequencer (ABI Prism 310; Invitrogen). All other chemicals were of the highest commercially available grade.

RESULTS

Identification of TAPL Homologues

Based on the conservation of many ABC transporters from bacteria to human, we predicted that similar members of TAPL might also be present in *C. elegans*. The previous phylogenetic study showed that TAPL, TAP1, and TAP2 constitute a single clade alongside with five *C. elegans* HAF proteins, HAF-2, HAF-4, HAF-7, HAF-8, and HAF-9, which had been originally identified as half-type ABCB proteins (Sheps *et al*., 2004). Among them, HAF-4 and HAF-9 are most homologous to TAPL; their identities to human TAPL are 38% in amino acid sequences, whereas those of HAF-2, HAF7, and HAF-8 to TAPL are 35, 31, and 34%, respectively. Both HAF-4 and HAF-9 are more homologous to TAPL than to TAP1 and TAP2; the identities to TAP1 are 28% (HAF-4) and 30% (HAF-9), and those to TAP2 are 30% (HAF-4) and 33% (HAF-9).

Both HAF-4 and HAF-9 have well-conserved nucleotide binding and hydrolysis motifs in the ABC domain, including a Walker A motif that contacts the α- and β-phosphates, a Walker B motif that contains a conserved glutamate, and a signature motif that interacts with γ-phosphates (Figure 1A). The phylogenetic tree based on the alignment using ABC domains of *C. elegans* and human half-type ABC B subfamily members also shows that the closest members of human TAPL are HAF-4 and HAF-9 (Figure 1B).

Moreover, HAF-4 and HAF-9 are similar to each other with 47% in the full length and 68% in the ABC domain being identical, and probably they are paralogues. They have a strong similarity in the ABC domain and the amino-terminal putative transmembrane domain but not in the carboxy-terminal amino acid sequences. In this study, we focused on both HAF-4 and HAF-9 as TAPL homologues.

Tissue-specific Expression of HAF-4 and HAF-9

Determination of the tissue distribution and subcellular localization of TAPL homologues provides information to elucidate their roles in *C. elegans*. We monitored the distribution of HAF-4 and HAF-9 in vivo using translational GFP fusion constructs. The HAF-4::GFP and HAF-9::GFP expressions were observed at the larval and adult stages exclusively in all of the 20 intestinal cells of which a whole intestine consists (Figure 2, A–D). At the embryonic stage, no expression of HAF-4::GFP or HAF-9::GFP was found (data not shown). These results are consistent with those of a previous report on the cyclopedic promoter analysis of *C. elegans* ABC B subfamily members (Zhao *et al*., 2004), in which the main organ expressing *haf-4* and *haf-9* is intestine.

HAF-4 and HAF-9 Localize in Nonacidic but LMP-1–positive Intestinal Granules

In intestinal cells of the late larval and adult stages, HAF-4::GFP and HAF-9::GFP seemed, under confocal microscopy, to be distributed on the surface of intestinal granules of some sort (Figure 2, E–H). Western blot analysis using polyclonal antiserum against the recombinant HAF-4 and HAF-9 proteins and anti-GFP antibody revealed that both GFP-tagged and endogenous proteins were enriched in the membrane fraction (Supplemental Figure 1). These results indicate that HAF-4 and HAF-9 are present on the membranes of some intestinal granules. The HAF-4::GFP-positive and HAF-9::GFP-positive granules were relatively large (>2 μm average diameter) and accounted for the majority of distinguishable intestinal granules. These granules were filled with neither autofluorescent nor birefringent contents. *C. elegans* intestinal cells are highly polarized; nonetheless

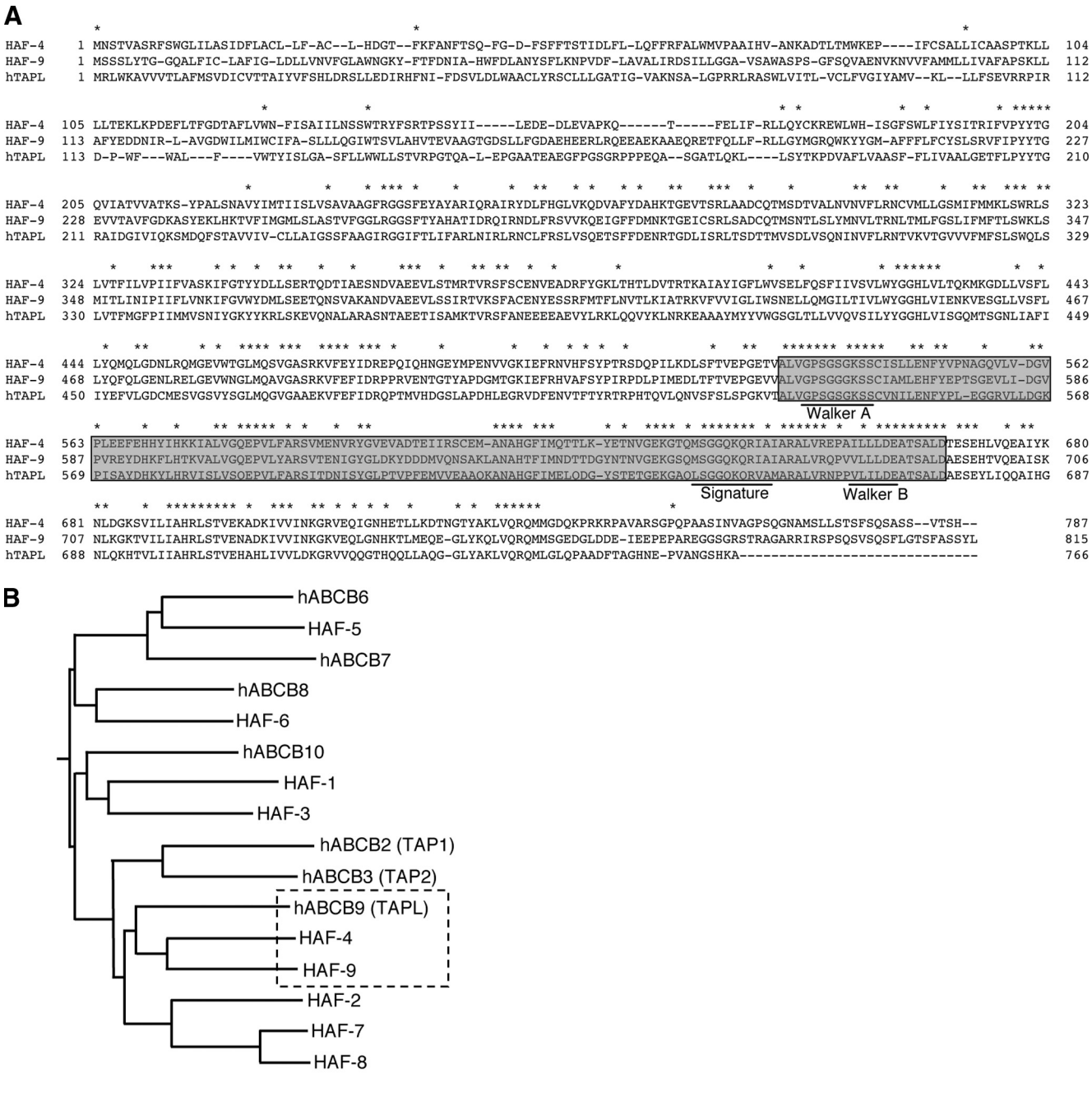

Figure 1. *C. elegans* HAF-4 and HAF-9 ABC transporter proteins highly homologous to human TAPL. (A) Comparison of the deduced amino acid sequences of *C. elegans* HAF-4 (NCBI accession number NP 001021666), HAF-9 (NP 871810), and human TAPL (Q9NP78). The ABC domains are indicated using a gray box. Walker A, Walker B, and signature motifs are underlined. Asterisks show identical amino acid residues. (B) Phylogenetic tree of *C. elegans* and human half-type ABCB proteins at the level of amino acid sequences of ABC domain. *C. elegans* has nine half-type ABCB proteins: HAF-1 (NP 503098), HAF-2 (NP 495537), HAF-3 (NP 506927), HAF-4, HAF-5 (also known as HMT-1, NP 001022812), HAF-6 (NP 490828), HAF-7 (NP 506645), HAF-8 (NP 502776), and HAF-9. Human has seven half-type ABCB proteins: ABCB2 (TAP1, Q03518), ABCB3 (TAP2, Q9UDX4), ABCB6 (Q9NP58), ABCB7 (O75027), ABCB8 (Q9NUT2), ABCB9 (TAPL), and ABCB10 (Q9NRK6). Their ABC domains were aligned using ClustalW program. Based on these alignments, a phylogenetic tree was constructed using the dendrogram method.

these granules were distributed evenly throughout the cytoplasm.

For characterization of HAF-4::GFP-positive and HAF-9::GFP-positive intestinal granules, we performed double labeling of intestinal cells with acridine orange, a dye for acidic compartment staining. As a result, HAF-4::GFP-positive and acridine orange-positive granules turned out to be mutually exclusive (Figure 3, A–C), and the pattern was same in case of HAF-9::GFP-positive granules (Figure 3, D–F). A similar exclusive pattern was observed when LysoTracker Red, another dye for monitoring the acidification of subcellular compartments, was used in place of acridine orange (Supplemental Figure 2A).

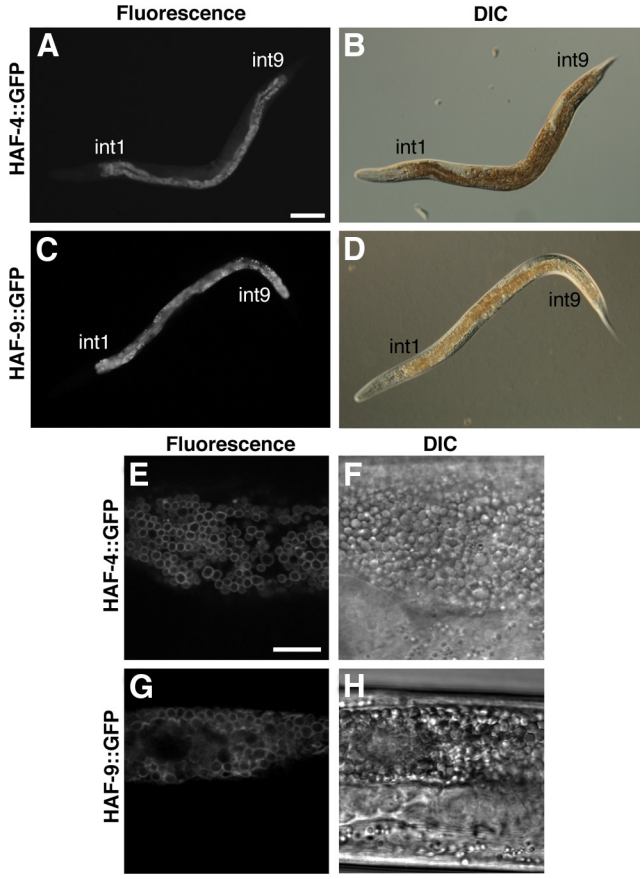

Figure 2. Intestinal expression of HAF-4 and HAF-9 in *C. elegans*. (A–D) GFP fluorescences (A and C) and the corresponding DIC images (B and D) of *Is*[*haf-4::GFP*] (A and B) and *Is*[*haf-9::GFP*] (C and D) transgenic worms. Bars, 100 μm. The GFP fluorescences of HAF-4::GFP and HAF-9::GFP are observed mainly in intestinal cells. (E–H) Confocal images of intestinal cells around the vulva of *Is*[*haf-4::GFP*] (E and F) and *Is*[*haf-9::GFP*] (G and H). GFP fluorescences (E and G) and the corresponding DIC images (F and H) are presented. Bars, 10 μm. Both HAF-4::GFP and HAF-9::GFP are clearly localized on the periphery of intestinal granules. Tiny white dots are autofluorescent granules; their fluorescence is not derived from GFP, according to spectral analysis.

Next, we performed coexpression of HAF-4::GFP and HAF-9::GFP with LMP-1, a *C. elegans* homologue of *l*ysosome-associated membrane protein (LAMP). The overlap of HAF-4::GFP and HAF-9::GFP with LMP-1::mRFP was detected in a subset of granules (Figure 3, G–L). In contrast, the lipid droplet staining with Nile Red, and the fluorescence of a mitochondrial marker HSP-60::mRFP did not overlap with that of HAF-4::GFP (Supplemental Figure 2, B and C). These results indicate that HAF-4::GFP localizes in nonacidic but lysosomal marker-positive intestinal granules.

We also demonstrated the effect of vesicular transport mutations, *rab-10(q373)* and *ppk-3(n2668)*, on HAF-4 and HAF-9 localizations (Figure 3, M–T). RAB-10 is a key regulator of endocytic recycling in *C. elegans* intestine (Chen *et al.*, 2006). In the intestine of *rab-10(q373)*, abnormally enlarged vacuoles were stained with RAB-5, an early endosome marker. Neither HAF-4::GFP nor HAF-9::GFP was located on the membrane of the enlarged vacuoles (Figure 3, M–P). PPK-3 is a homologue of phosphoinositide kinase PIKfyve/Fab1p in *C. elegans* and regulates the formation of terminally maturated nonacidic late lysosome. In the intestine of *ppk-3(n2668)*, a hypomorphic mutant of the PPK-3 kinase domain (Nicot *et al.*, 2006), abnormally enlarged vacuoles were stained with LMP-1. HAF-4::GFP and HAF-9::GFP were also located on the membrane of the enlarged vacuoles in the intestine of *ppk-3(n2668)* (Figure 3, Q–T). These results indicate that HAF-4 and HAF-9, like LMP-1, are localized in terminally maturated late lysosome but in neither early endosome nor acidified lysosome.

Intestinal Granular Loss in Deletion Mutants for haf-4 and haf-9

To investigate the function of these TAPL homologue genes, we analyzed deletion mutants available from the *Caenorhabditis* Genetics Center (Figure 4A). Using microscopic observation, we found the intestinal granular loss in the *haf-4* and *haf-9* deletion mutants from the late larval to young adult stage. DIC microscopy revealed that intestinal cells of wild-type N2 worms were filled with granules (Figure 4B). However, *haf-4(ok1042)*, *haf-4(gk240)*, and *haf-9(gk23)* contained lesser quantities of large intestinal granules except for autofluorescent and birefringent granules (Figure 4, C–E). This was similar to *lmp-1(nr2045)* (Figure 4G). In the deletion mutant for *haf-2*, which shows the highest identity (35% at the amino acid level) to human TAPL next to HAF-4 and HAF-9, no intestinal defects were observed (Figure 4F). Other *haf* mutants, such as the *haf-2* mutant, showed no obvious intestinal granular defects (Supplemental Figure 3). *lmp-1(nr2045)* was found to engender drastic alteration in intestinal granule populations with apparent loss of acridine orange stain-negative granules (Kostich *et al.*, 2000). Therefore, we also performed dye staining with acridine orange in wild-type and the *haf-4* deletion mutant worms, and the results suggest that lost granules in the *haf-4* mutants were nonacidic granules without autofluorescence (Supplemental Figure 4).

The granular loss was apparent in the middle intestinal cells close to the vulva, such as int5, but not in int1. Int1 cells contained higher amounts of autofluorescent granules than did other intestinal cells; therefore, the nonautofluorescent large granular loss might not be prominent in int1. At the adult stage, the granules lost in the mutants were gradually formed as the worm aged and no gross phenotype was found in 1-wk adults any more. Therefore, this granular loss is a stage-specific transient phenotype. These defects were observed in the homozygous mutants but not in the heterozygous mutants (data not shown). The average diameter of lost granules was >2 μm, which was 10- to 20-fold larger than that of peroxisome reported in a previous study (Togo *et al.*, 2000).

The intestinal subcellular localization of HAF-4 and HAF-9 coincided with that of LMP-1 and the granular loss phenotype in the *haf-4* and *haf-9* mutants resembled that in the *lmp-1* deletion mutant at the DIC level. Therefore, we performed transmission electron microscopic analysis to investigate the ultrastructure of the *haf-4*, *haf-9*, and *lmp-1* mutants further. Observation at the electron microscopic level revealed ultrastructural differences in the population and shape of intracellular granules between *lmp-1* and *haf-4* (Figure 4, H–K). The intestinal cells of wild-type N2 worms were full of granules stained in gray (Figure 4H). However, those granules disappeared in the *haf-4* and *haf-9* mutant worms, whereas white or small dark granules were remaining (Figure 4, I and J, respectively). Conversely, the *lmp-1* mutant worms had deformed and bumpy masses of granules with fusion (Figure 4K). The small dark granules seem to be lipid-containing acidic granules that are both Nile Red

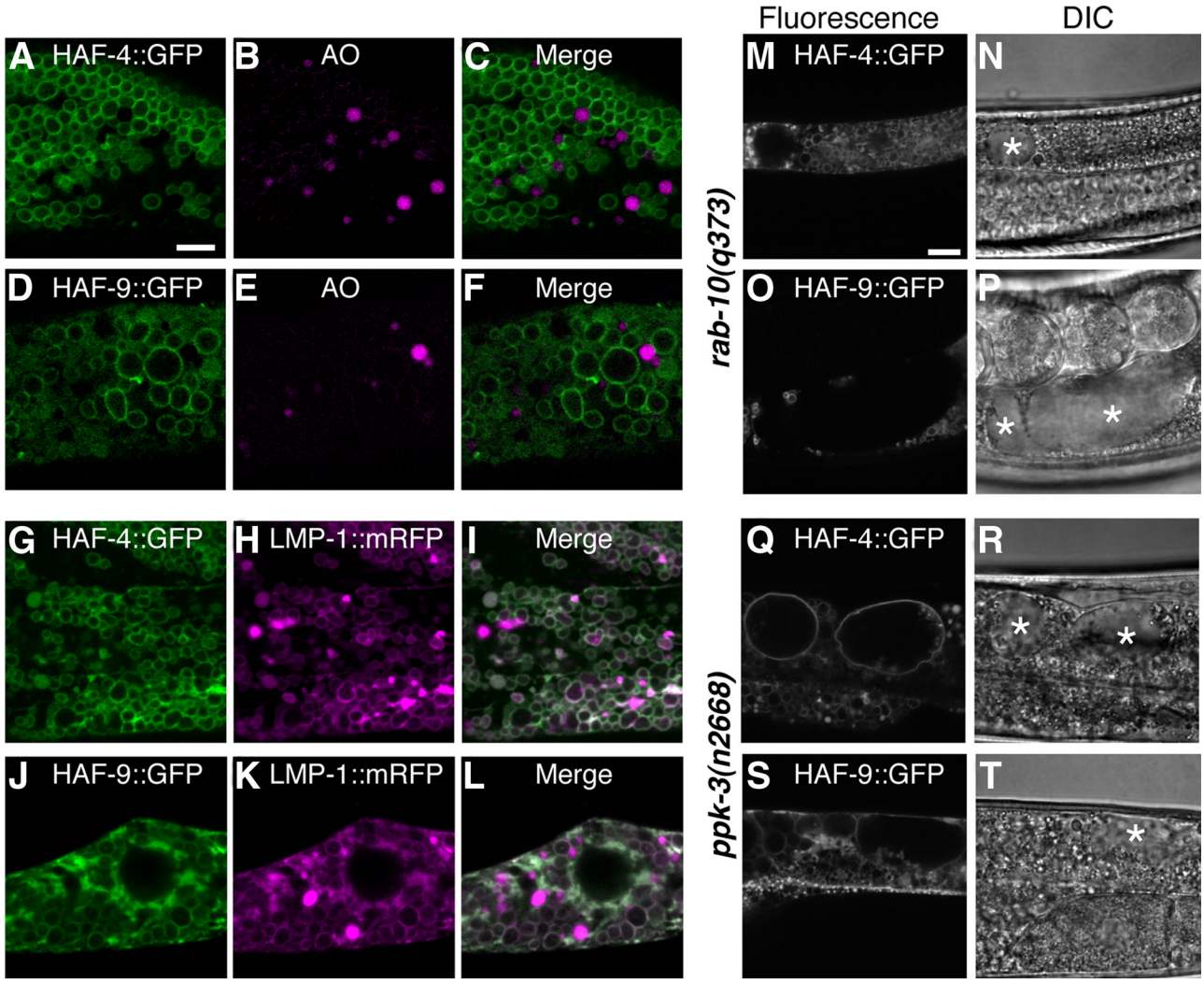

Figure 3. HAF-4::GFP– and HAF-9::GFP–positive granules are nonacidic, but LMP-1–positive intestinal granules. (A–F) Staining of *Is*[*haf-4::GFP*] (A–C) and *Is*[*haf-9::GFP*] (D–F) transgenic worms with acridine orange, a dye for acidic compartment labeling. GFP in green (A and D), acridine orange in magenta (B and E), and the merged images (C and F). Fluorescence from GFP and acridine orange is unmixed by λ-scanning with a confocal microscope. Neither HAF-4::GFP– nor HAF-9::GFP–positive granules overlap with acridine orange-positive granules. (G–L) Coexpression of HAF-4::GFP (G) or HAF-9::GFP (J) with organelle marker LMP-1::mRFP (H and K), which is a *C. elegans* homologue of a mammalian lysosomal protein LAMP. As shown in the merged images (I and L), HAF-4::GFP and HAF-9::GFP are mostly colocalized with LMP-1::mRFP. Bars, 5 μm. (M–T) Subcellular localization of HAF-4::GFP and HAF-9::GFP in the vesicular transport-defective mutants. Bars, 10 μm. Neither HAF-4::GFP (M and N) nor HAF-9::GFP (O and P) are localized on the abnormally enlarged early endosome characteristic of *rab-10(q373)* (M–P). In contrast, they are observed on the edge of enlarged vacuoles in *ppk-3(n2668)*, which reportedly accumulates LMP-1–positive large vacuoles (Q–T). The enlarged vacuoles in the DIC images are traced with asterisks (N, P, R, and T).

positive and acridine orange positive. These granules were still observed in the *haf-4*, *haf-9*, and *lmp-1* mutants.

Defects of LMP-1::mRFP–positive Granules in Deletion Mutants for haf-4 and haf-9

LMP-1 colocalized with HAF-4 and HAF-9 on the surface of nonacidic intestinal granules (Figure 3, G–L); thus, we next investigated the subcellular localization of LMP-1 in the deletion mutants for *haf-4* or *haf-9* to decipher the mechanism of intestinal granular loss (Figure 5). LMP-1::mRFP was detected in a subset of nonacidic granules in wild-type N2 (Figure 5, A and B); however, in the *haf-4* mutants it was not detected on the surface of visible granules but showed the web-like localization (Figure 5, C–F). The LMP-1::mRFP fluorescence signal was concentrated close to apical lumen. We observed a similar fluorescence pattern of LMP-1::mRFP in the *haf-9* mutant (Figure 5, G and H). These results indicate that lost granules in the *haf-4* and *haf-9* mutants are LMP-1–positive granules, and are probably also HAF-4 and HAF-9 positive.

Rescue of the Intestinal Granular Defect of the haf-4 and haf-9 Deletion Mutants by HAF-4::GFP and HAF-9::GFP Expression

It was strongly expected that the lost granules in the *haf-4* and *haf-9* mutants were HAF-4– and HAF-9–expressing granules in normal worms. To examine whether HAF-4 is necessary for the granular formation, we next performed a rescue experiment of intestinal granular phenotype observed in the *haf-4* deletion mutants by introduction of the

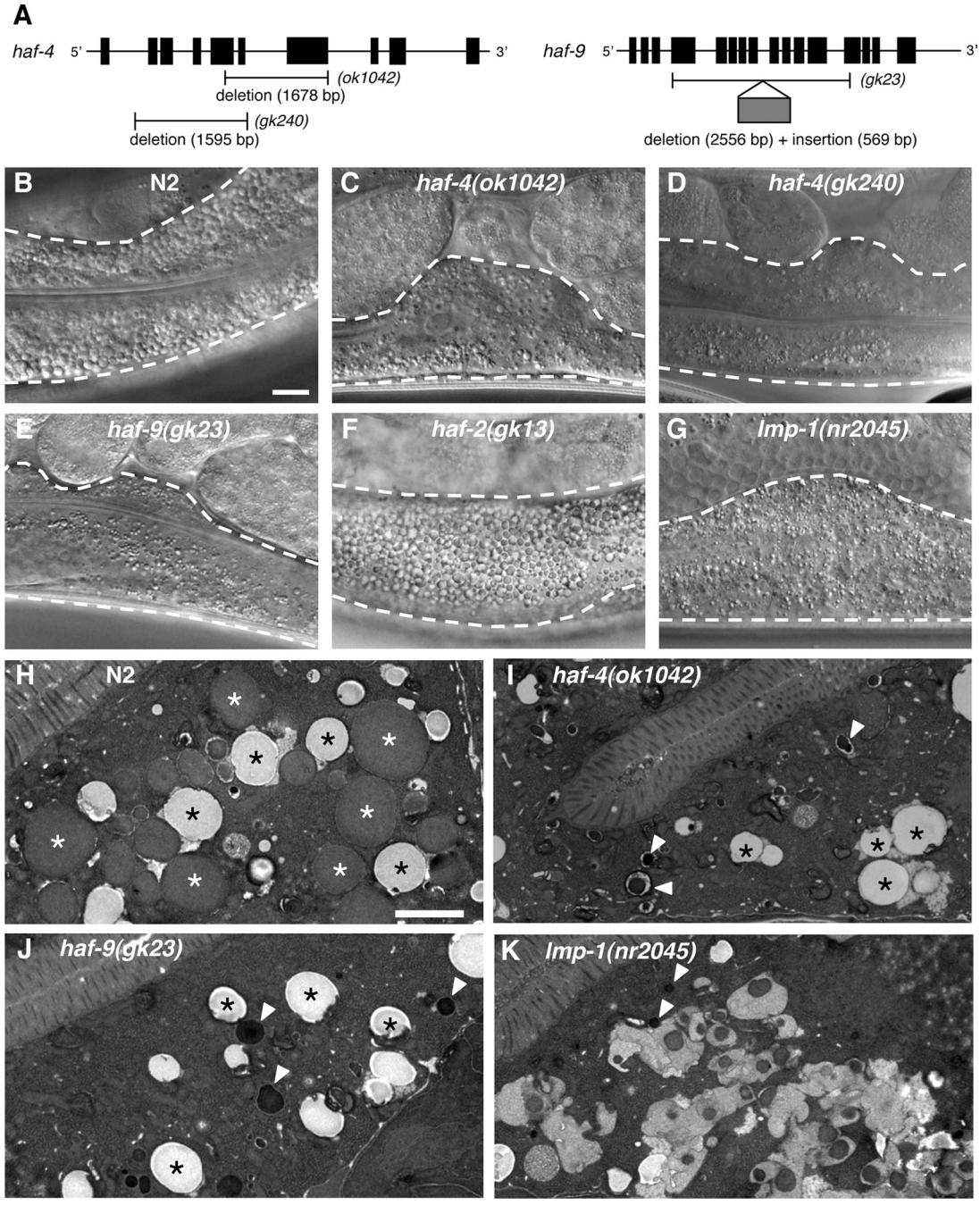

Figure 4. Loss of large intestinal granules in the *haf-4* and *haf-9* mutants at the young adult stage. (A) Schematic representations of the genome structures of the *haf-4* and *haf-9* genes and their mutants. Black boxes on each gene delineate exons. The position and length of deletion and/or insertion found in the mutants are indicated with bars below the genome structures. (B–G) DIC images of intestinal cells near the vulva in wild-type N2 (B), *haf-4(ok1042)* (C), *haf-4(gk240)* (D), *haf-9(gk23)* (E), *haf-2(gk13)* (F), and *lmp-1(nr2045)* (G). Bar, 10 μm. Intestinal cells are tightly packed with granules in wild-type and the *haf-2* mutant (B and F), whereas the *haf-4*, *haf-9*, and *lmp-1* mutants have lost numerous such granules (C, D, E, and G). Statistical analysis of granular numbers in each strain are provided in Figure 6M. (H–K) Electron micrographs of the intestine of a wild-type worm and mutants with intestinal granular defects. All cross sections were prepared from the young adult. In the wild-type N2 section (H), most intestinal cell areas are occupied by gray large granules (~2 μm in diameter), as indicated by white asterisks. In *haf-4(ok1042)* (I), *haf-4(gk240)* (data not shown), and *haf-9(gk23)* (J); however, those large granules have entirely disappeared, and both white granules and small dark granules remain as indicated by black asterisks and open arrowheads, respectively. In *lmp-1(nr2045)* (K), in addition to the loss of large gray granules same as the *haf-4* and *haf-9* mutants, granule fusion is observed, as reported by Kostich *et al*. (2000). Bar, 2 μm.

haf-4 transgene. Expression of HAF-4::GFP driven by its own promoter resulted in the recovery of most of the intestinal granules lost in *haf-4(ok1042)* (Figure 6, A and B) to the comparable level of wild type (Figure 2, E and F). The phenotype of another *haf-4* mutant *haf-4(gk240)* was also rescued by exogenous HAF-4::GFP (Figure 6, C and D).

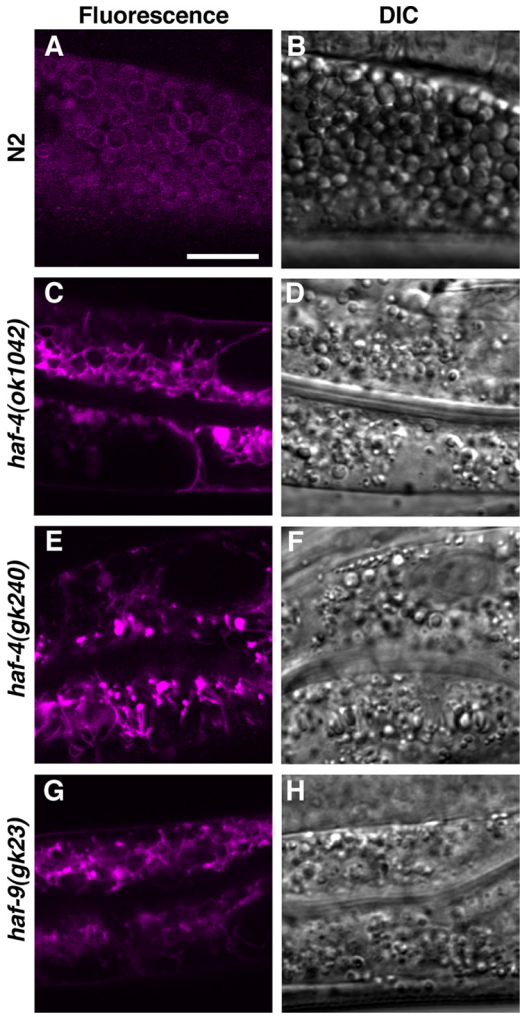

Figure 5. Defective formation of LMP-1::mRFP–positive intestinal granules in the *haf-4* and *haf-9* mutants. (A–H) *Is*[*Pges-1::lmp-1::mRFP*] in the wild-type background (A and B) was crossed with *haf-4(ok1042)* (C and D), *haf-4(gk240)* (E and F), and *haf-9(gk23)* (G and H). mRFP fluorescences (A, C, E, and G) and corresponding DIC images (B, D, F, and H). In these three mutants, LMP-1::mRFP shows the web-like intracellular localization unlike wild type. Autofluorescence was below the detectable level in the *haf-4* and *haf-9* mutants. Bars, 10 μm.

However, expression of HAF-4(K539M)::GFP, an inactive form of HAF-4 with the mutation in the Walker A motif, did not rescue the phenotype (Figure 6, E–H). The corresponding mutation of TAP interferes with peptide transfer (Lapinski *et al*., 2001) and in case of TAPL, the mutation results in the loss of ATP-binding activity and drug resistance sensitivity in yeast (Ohashi-Kobayashi *et al*., 2006; Ohara *et al*., 2008). These results suggest that the transport activity of HAF-4 was necessary for the formation or maintenance of intestinal granules in which HAF-4 itself located. Moreover, even in the wild-type N2 background, the distribution of overexpressed HAF-4(K539M)::GFP is patchy, of small dots, suggesting that the mutation in ATP-binding site of HAF-4 inhibits the maturation of granules as dominant-negative effects (Figure 6, I and J). Expression of HAF-9::GFP driven by its own promoter also rescued the granular loss phenotype in *haf-9(gk23)* (Figure 6, K and L). These results were supported by the statistical analysis of the granular numbers as shown in Figure 6M.

Slow Growth and Other Phenotypes

The intestine is the primary organ of nutritional interface, energy stores and front line defense (McGhee, 2007). At first, we expected some visible phenotype of the *haf-4* and *haf-9* mutants but no gross defects were observed in body form, body size, and movement of adult worms of these mutants. The intestine performs yolk protein synthesis for gonad development (Kimble and Sharrock, 1983); therefore, we examined the brood size of these deletion mutants. As a result, the *haf-4* and *haf-9* deletion mutants showed slight but significant defects on the brood size of hermaphrodites (Figure 7A).

While maintaining these strains, we noticed that the *haf-4* and *haf-9* mutants had the slow growth phenotype (Figure 7B). Compared with wild-type worms, the *haf-4* and *haf-9* homozygous mutants were almost 10 h late in becoming adults from fresh-laid eggs at 20°C. In contrast, the *haf-2* homozygous mutant grew at almost the normal rate.

Possibly, the slow growth resulted from some mechanical problem in the alimentary canal. For that reason, we examined the pharyngeal pumping and defecation rate. Results showed that the *haf-4* and *haf-9* deletion mutant worms had a similar pumping rate to wild-type. In contrast, these mutants showed a defecation rate defect. [Wild-type N2 47.3 $\pm$ 2.9 s ($n = 3$ with at least 10 measurements for each worm), *haf-4(ok1042)* 59.3 $\pm$ 1.5 s ($n = 5$, $p < 0.005$), *haf-4(gk240)* 61.7 $\pm$ 5.3 s ($n = 7$, $p < 0.0005$), *haf-9(gk23)* 62.5 $\pm$ 6.2 s ($n = 4$, $p < 0.01$)].

DISCUSSION

This article described tissue distribution, subcellular localization, and several mutant phenotypes of *C. elegans* TAPL homologues, HAF-4 and HAF-9. As shown in the first part of this article, the colocalization of HAF-4 and HAF-9 with LMP-1 in intestinal granular organelles may indicate a functional relation to mammalian TAPL, which localizes with LAMPs in lysosome but has unknown functions in vivo (Zhang *et al*., 2000; Kamakura *et al*., 2008). Interestingly, the intestinal granules in which these proteins locate are not acidic. These results raise a possibility that a specific granular population of "nonacidic lysosomes" resides in *C. elegans* intestine. The phrase "nonacidic lysosomes" may sound paradoxical because lysosome is defined normally as an acidic intracellular compartment; and in fact, in coelomocytes, macrophage-like scavenger cells of *C. elegans* migrating in pseudocoelom, LMP-1–positive granules are acidified (Nicot *et al*., 2006). However, in *C. elegans* intestinal cells at the late larval and adult stages, other LMP-1–negative acidic granules with autofluorescent contents, so-called lipofuscin granules or secondary lysosome, do exist (Clokey and Jacobson, 1986; Hermann *et al*., 2005). Diverse functions of lysosome and lysosome-related organelles are now reported from many organisms (Dell'Angelica *et al*., 2000). The *C. elegans* intestine possesses lysosome or lysosome-related organelles of several different types whose classification and identification have not been completed. According to our results of the HAF-4 and HAF-9 localization in mutants with vesicular transport defect, *rab-10* and *ppk-3*, they localize not on early endosome but on "late lysosome," which have been described as the nonacidic LMP-1–positive granules participating in membrane retrieval (Nicot *et al*., 2006). Interestingly, LMP-1 has been shown to localize on the enlarged vacuoles in both the *ppk-3* and *rab-10* mutants unlike HAF-4 and HAF-9, suggesting that early endosome is LMP-1 positive but HAF-4/9 negative. Although the existence of such an

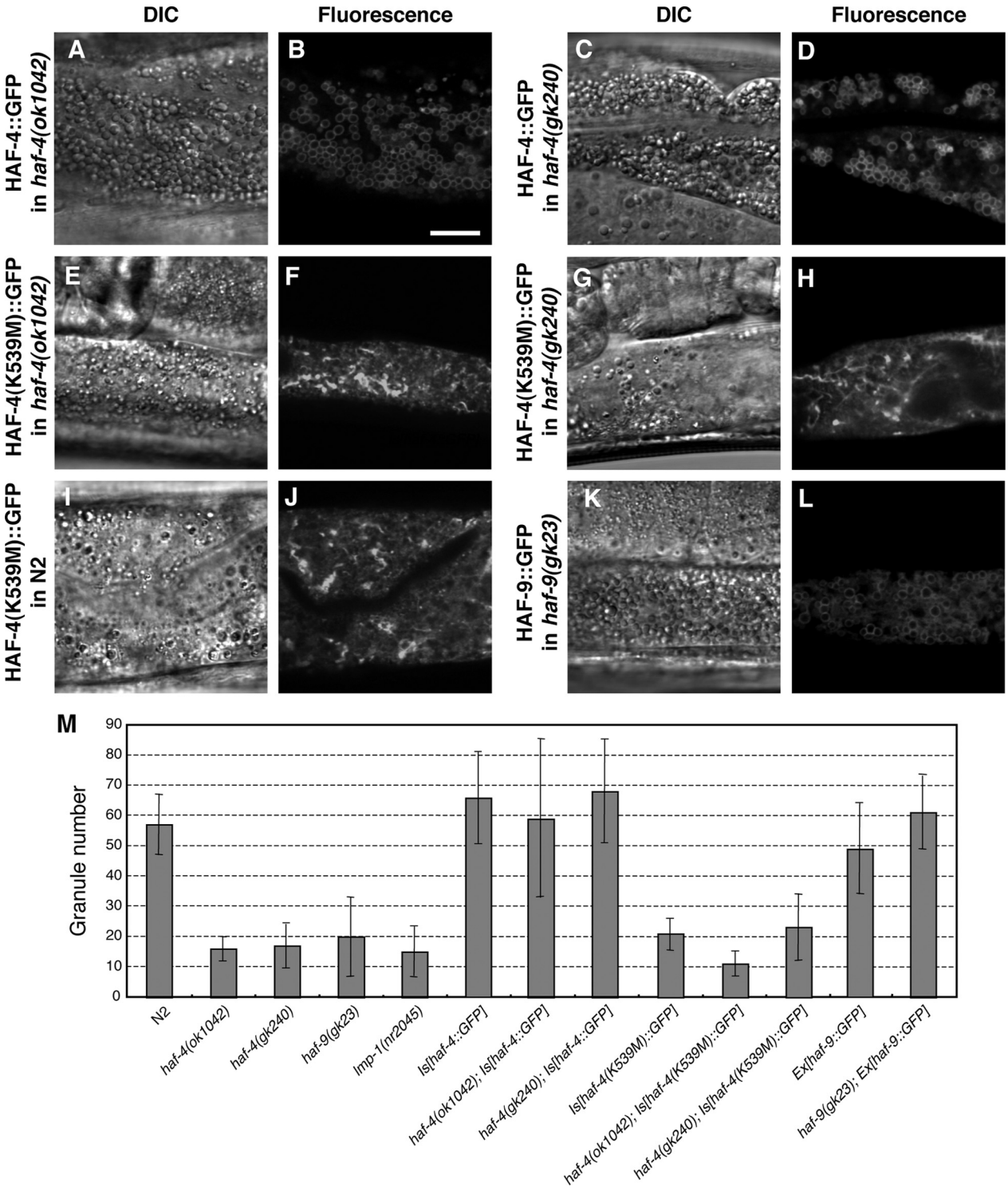

Figure 6. Intestinal granular loss phenotype of the *haf-4* mutant was rescued by HAF-4::GFP, but not by HAF-4::GFP(K539M) with a mutation in the Walker A motif. (A and B) In *haf-4(ok1042);Is*[*haf-4::GFP*], the HAF-4::GFP–positive granules are recovered to the extent comparable to wild type (see Figure 2, E and F). (C and D) Identical result is obtained in *haf-4(gk240);Is*[*haf-4::GFP*]. (E–H) In both *haf-4(ok1042);Is*[*haf-4(K539M)::GFP*] (E and F) and *haf-4(gk240);Is*[*haf-4(K539M)::GFP*] (G and H), the phenotype by the *haf-4* mutation is not rescued. HAF-4(K539M)::GFP seems to aggregate and distribute within cytoplasm. (I and J) Even in the wild-type N2 background, HAF-4(K539M)::GFP engenders abnormal formation of intestinal granules. (K and L) In *haf-9*, the HAF-9::GFP–positive granules are also recovered in *haf-9(gk23);Ex*[*haf-9::GFP*]. Bar, 10 μm. (M) Quantification of intestinal granules. The numbers of granules with diameter of 1 μm or more in 300 μm^2 on DIC images were manually counted. Five worms for each strain were subjected to the analysis. The granular number decreased significantly against N2 in *haf-4(ok1042)*, *haf-4(gk240)*, *haf-9(gk23)*, *lmp-1(nr2045)*, *Is*[*haf-4(K539M)::GFP*], *haf-4(ok1042);Is*[*haf-4(K539M)::GFP*], and *haf-4(gk240);Is*[*haf-4(K539M)::GFP*]) ($p < 0.001$). In contrast, the granular number was comparable to N2 with no significance in *Is*[*haf-4::GFP*], *haf-4(ok1042);Is*[*haf-4::GFP*], *haf-4(gk240);Is*[*haf-4::GFP*], *Ex*[*haf-9::GFP*], and *haf-9(gk23);Ex*[*haf-9::GFP*] ($p > 0.1$). The difference in the granular number between the *haf-4* or *haf-9* mutant strains and those rescued by HAF-4::GFP or HAF-9::GFP was significant in all cases ($p < 0.05$).

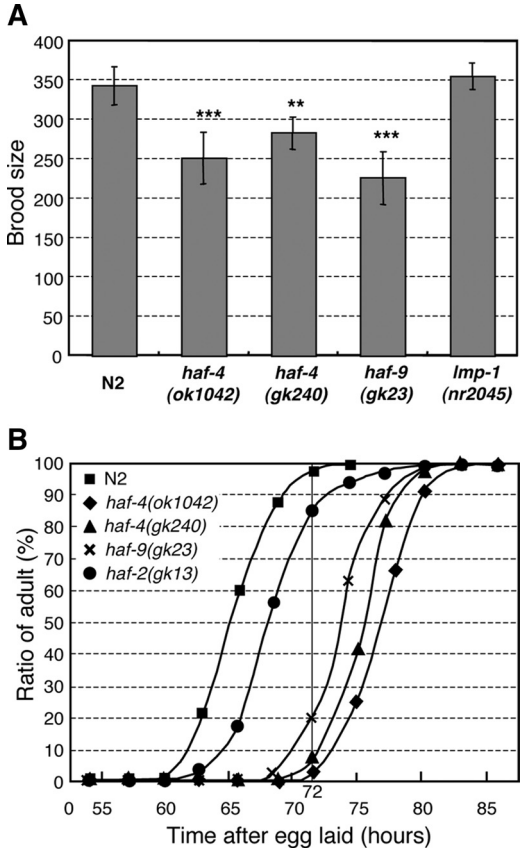

Figure 7. The *haf-4* and *haf-9* mutants show reduced brood size and slow growth phenotypes. (A) Brood size of the *haf-4* and *haf-9* mutants. Ten worms for each strain were subjected to the analysis. $^{**}p < 0.01$. $^{***}p < 0.001$. These *haf* mutants showed significantly-reduced brood size, whereas *lmp-1(nr2045)* did not. (B) Comparison of time to reach adulthood. After eggs were laid on NG agar plates, the worms which reached adulthood on the plates were counted every 3 h [n = 448 (N2), 689 (*haf-4(ok1042)*), 779 (*haf-4(gk240)*), 635 (*haf-9(gk23)*), 639 (*haf-2(gk13)*)]. Almost all wild-type worms grew to adults at 72 h after egg laid, although <20% of the *haf-4* and *haf-9* mutants became adults at the time ($p < 0.001$). It took almost 10 h longer for all the *haf-4* and *haf-9* homozygous mutants examined to become adults than the wild-type worms. The *haf-2* mutant also showed slow growth phenotype but the defect was slight compared with those of the *haf-4* and *haf-9* mutants.

organelle was not clearly detected in the wild-type background, probably due to its minor population, these findings imply the differential dynamics between LMP-1 and HAF-4/9 in membrane trafficking to the same destination.

We next described novel intestinal granular defects in deletion mutants for *haf-4* and *haf-9*, and determined that HAF-4 and HAF-9 are required for the formation and/or maturation of nonacidic LMP-1–positive granules. The granular defects observed in the *haf-4* and *haf-9* mutants were obviously different from those in the *lmp-1* mutant and recently reported *tat-1* mutant (Ruaud *et al*., 2009) under a transmission electron microscope in that *lmp-1* and *tat-1* showed aberrant membrane-limited vacuoles, which are never found in *haf-4* and *haf-9*. Recently, deficiency of two other *C. elegans* ABC transporters, PGP-2 and MRP-4, was reported to cause abnormality in other types of intestinal granules. Disrupting the function of PGP-2, a well-characterized ABCB subfamily member in *C. elegans*, results in the loss of acidic granules in embryonic and adult intestinal cells (Ashrafi *et al*., 2003; Nunes *et al*., 2005; Schroeder *et al*., 2007). The function of MRP-4 in the biogenesis of an intestinal lysosome-related fat storage organelle with birefringent and autofluorescent contents also has been reported previously (Currie *et al*., 2007). Therefore, several ABC transporters seem to be related to organelle biogenesis of different types, perhaps dependent on their distinct biochemical properties.

Then, how do two ABC transporters, HAF-4 and HAF-9, function for the formation and maintenance of LMP-1–positive nonacidic granules? Our results suggest that the intestinal phenotype of the *haf-4* mutants is relevant to the ATP-binding activity of HAF-4. Consequently, its transport activity seems to be necessary for enlargement of the granules. Although the substrates of HAF-4 and HAF-9 have not been elucidated, similarity to TAPL suggests that HAF-4 and HAF-9 transport peptides from cytosol to the granules. The peptides transported by HAF-4 and HAF-9 may somehow contribute to the normal formation of the granules.

As shown for other half-type ABC transporters examined to date, including TAP1/2 heterodimer and TAPL homodimer (Leveson-Gower *et al*., 2004; Ohara *et al*., 2008), it is likely that HAF-4 and HAF-9 function as a dimer. One possibility is that HAF-4 and HAF-9 function as a homodimer: consequently, the overexpression of the mutated HAF-4, HAF-4(K539M), would dominantly inhibit the function of the endogenous HAF-4. Another possible model is that HAF-4 forms a heterodimer with HAF-9. The latter model is supported by the result that mutation of *haf-9* renders the same phenotypes as *haf-4*. In this case, the mutant form of HAF-4 would inhibit HAF-4/HAF-9 transporters by binding competitively with HAF-9. These two possibilities do not need to be mutually exclusive. Further biochemical and genetic analyses are expected to clarify the relationship between HAF-4 and HAF-9.

In addition to the intestinal granular defect, we reported other phenotypes, reduced brood size, slow growth, and longer defecation cycles in the *haf-4* and *haf-9* deletion mutants. It is a natural question whether these phenotypes are attributable to the intestinal granular defect. The expression of both HAF-4 and HAF-9 is restricted in the intestine from larval to adult stage, which supplies nutrients to other tissues by secreting them to pseudocoelom. Furthermore, the large granules lost in the *haf-4* and *haf-9* mutant adults resemble yolk-containing intestinal granules described in WormAtlas (Altun and Hall, 2005), although their identity is still controversial and the precise pathway of yolk protein transport in intestinal cells has not been clarified. Together, HAF-4– and HAF-9–positive granules may participate in the storage and transport of the nutrients including peptidic substrates for HAF-4 and HAF-9. Possibly, the function of HAF-4 and HAF-9 at the larval stage is required for the normal growth rate and spermatogenesis; the expression at the adult stage may lead to the proper oogenesis. The defect in defecation cycles is thought to be associated with the reduction of nutrient availability in intestine (Thomas, 1990).

Interestingly, we observed a decrease in the HAF-4–positive granules when larval and adult worms were starved for a few hours (unpublished data). Possibly, peptides digested from food as nutrients would be reduced, and the absence of transport substrates of HAF-4 and HAF-9 might rapidly inhibit the formation of the proper enlarged granules observed in nutrient-rich conditions.

In conclusion, we demonstrated that *C. elegans* TAPL homologues function for intestinal granule formation and several physiological aspects related to the nutrition availability and the growth rate. Furthermore, the transport activity of HAF-4 probably affects the normal formation of intestinal

granules. We propose the possibility that HAF-4 and HAF-9 sustain the normal growth of worms by transporting putative nutrient peptides into granules via these transporters. Although our model remains hypothetical, further characterization of HAF-4– and HAF-9–positive intestinal granules as well as the identification of the substrates of HAF-4 and HAF-9 will provide insights into not only the physiological role of nonacidic lysosome-related organelles in *C. elegans* intestine but also an ancestral function of lysosomal ABC transporters.

ACKNOWLEDGMENTS

We thank Shin-ichirou Hori, Hiroko Iseoka, and Wei-Bin Du for help in early stages of this work. We profoundly appreciate Dr. Toshihiko Oka for providing useful suggestions and materials. Some nematode strains used in this work also were provided by Dr. Jocelyn Laporte and the *Caenorhabditis* Genetics Center, which is funded by the National Institutes of Health National Center for Research Resources. Plasmid vectors were kindly provided by Dr. Andrew Fire (Stanford University, Stanford, CA). This research was supported in part by grants from Ministry of Education, Culture, Sports, Science and Technology [Grants-in-Aid for Scientific Research C (13672284) and C (19590066)] (to A.O.-K.) and Japan Society for the Promotion of Science [Grant-in-Aid for Scientific Research on Priority Areas B (13142206)] (to M. M.).

REFERENCES

Altun, Z. F., and Hall, D. H. (2005). Alimentary system (part II) the intestine. WormAtlas. (http://www.wormatlas.org/handbook/alimentary/alimentary2.htm).

Ashrafi, K., Chang, F. Y., Watts, J. L., Fraser, A. G., Kamath, R. S., Ahringer, J., and Ruvkun, G. (2003). Genome-wide RNAi analysis of *Caenorhabditis elegans* fat regulatory genes. Nature *421*, 268–272.

Brenner, S. (1974). The genetics of *Caenorhabditis elegans*. Genetics *77*, 71–94.

Broeks, A., Gerrard, B., Allikmets, R., Dean, M., and Plasterk, R. H. (1996). Homologues of the human multidrug resistance genes MRP and MDR contribute to heavy metal resistance in the soil nematode *Caenorhabditis elegans*. EMBO J. *15*, 6132–6143.

C. elegans Sequencing Consortium (1998). Genome sequence of the nematode *C. elegans*: a platform for investigating biology. Science *282*, 2012–2018.

Chen, C. C., Schweinsberg, P. J., Vashist, S., Mareiniss, D. P., Lambie, E. J., and Grant, B. D. (2006). RAB-10 is required for endocytic recycling in the *Caenorhabditis elegans* intestine. Mol. Biol. Cell *17*, 1286–1297.

Clokey, G. V., and Jacobson, L. A. (1986). The autofluorescent "lipofuscin granules" in the intestinal cells of *Caenorhabditis elegans* are secondary lysosomes. Mech. Ageing Dev. *35*, 79–94.

Currie, E., King, B., Lawrenson, A. L., Schroeder, L. K., Kershner, A. M., and Hermann, G. J. (2007). Role of the *C. elegans* multidrug resistance gene, mrp-4, in gut granule differentiation. Genetics *177*, 1569–1582.

Dean, M., and Annilo, T. (2005). Evolution of the ATP-binding cassette (ABC) transporter superfamily in vertebrates. Annu. Rev. Genomics Hum. Genet. *6*, 123–142.

Dell'Angelica, E. C., Mullins, C., Caplan, S., and Bonifacino, J. S. (2000). Lysosome-related organelles. FASEB J. *14*, 1265–1278.

Demirel, O., Waibler, Z., Kalinke, U., Grunebach, F., Appel, S., Brossart, P., Hasilik, A., Tampe, R., and Abele, R. (2007). Identification of a lysosomal peptide transport system induced during dendritic cell development. J. Biol. Chem. *282*, 37836–37843.

Gengyo-Ando, K., Yoshina, S., Inoue, H., and Mitani, S. (2006). An efficient transgenic system by TA cloning vectors and RNAi for *C. elegans*. Biochem. Biophys. Res. Commun. *349*, 1345–1350.

Hermann, G. J., Schroeder, L. K., Hieb, C. A., Kershner, A. M., Rabbitts, B. M., Fonarev, P., Grant, B. D., and Priess, J. R. (2005). Genetic analysis of lysosomal trafficking in *Caenorhabditis elegans*. Mol. Biol. Cell *16*, 3273–3288.

Higgins, C. F. (1992). ABC transporters: from microorganisms to man. Annu. Rev. Cell Biol. *8*, 67–113.

Imai, Y., Matsushima, Y., Sugimura, T., and Terada, M. (1991). A simple and rapid method for generating a deletion by PCR. Nucleic Acids Res. *19*, 2785.

Kamakura, A., Fujimoto, Y., Motoashi, Y., Ohashi, K., Ohashi-Kobayashi, A., and Maeda, M. (2008). Functional dissection of transmembrane domains of human TAP-like (ABCB9). Biochem. Biophys. Res. Commun. *377*, 847–851.

Kimble, J., and Sharrock, W. J. (1983). Tissue-specific synthesis of yolk proteins in *Caenorhabditis elegans*. Dev. Biol. *96*, 189–196.

Kleijmeer, M. J., Kelly, A., Geuze, H. J., Slot, J. W., Townsend, A., and Trowsdale, J. (1992). Location of MHC-encoded transporters in the endoplasmic reticulum and cis-Golgi. Nature *357*, 342–344.

Kobayashi, A., *et al*. (2000). A half-type ABC transporter TAPL is highly conserved between rodent and man, and the human gene is not responsive to interferon-γ in contrast to TAP1 and TAP2. J. Biochem. *128*, 711–718.

Kobayashi, A., Hori, S., Suita, N., and Maeda, M. (2003). Gene organization of human transporter associated with antigen processing-like (TAPL, ABCB9): analysis of alternative splicing variants and promoter activity. Biochem. Biophys. Res. Commun. *309*, 815–822.

Kostich, M., Fire, A., and Fambrough, D. M. (2000). Identification and molecular-genetic characterization of a LAMP/CD68-like protein from *Caenorhabditis elegans*. J. Cell Sci. *113*, 2595–2606.

Kurz, C. L., Shapira, M., Chen, K., Baillie, D. L., and Tan, M. W. (2007). Caenorhabditis elegans pgp-5 is involved in resistance to bacterial infection and heavy metal and its regulation requires TIR-1 and a p38 map kinase cascade. Biochem. Biophys. Res. Commun. *363*, 438–443.

Lapinski, P. E., Neubig, R. R., and Raghavan, M. (2001). Walker A lysine mutations of TAP1 and TAP2 interfere with peptide translocation but not peptide binding. J. Biol. Chem. *276*, 7526–7533.

Leveson-Gower, D. B., Michnick, S. W., and Ling, V. (2004). Detection of TAP family dimerizations by an *in vivo* assay in mammalian cells. Biochemistry *43*, 14257–14264.

Lindblom, T. H., Pierce, G. J., and Sluder, A. E. (2001). A *C. elegans* orphan nuclear receptor contributes to xenobiotic resistance. Curr. Biol. *11*, 864–868.

Mahajan-Miklos, S., Tan, M. W., Rahme, L. G., and Ausubel, F. M. (1999). Molecular mechanisms of bacterial virulence elucidated using a *Pseudomonas aeruginosa-Caenorhabditis elegans* pathogenesis model. Cell *96*, 47–56.

McGhee, J. D. (2007). The *C. elegans* intestine. WormBook. ed. The *C. elegans* Research Community. (http://www.wormbook.org).

Mello, C. C., Kramer, J. M., Stinchcomb, D., and Ambros, V. (1991). Efficient gene transfer in *C. elegans*: extrachromosomal maintenance and integration of transforming sequences. EMBO J. *10*, 3959–3970.

Mitani, S. (1995). Genetic regulation of *mec-3* gene expression implicated in the specification of the mechanosensory neuron cell types in *Caenorhabditis elegans*. Dev. Growth Diff. *37*, 551–557.

Nicot, A. S., Fares, H., Payrastre, B., Chisholm, A. D., Labouesse, M., and Laporte, J. (2006). The phosphoinositide kinase PIKfyve/Fab1p regulates terminal lysosome maturation in *Caenorhabditis elegans*. Mol. Biol. Cell *17*, 3062–3074.

Nunes, F., Wolf, M., Hartmann, J., and Paul, R. J. (2005). The ABC transporter PGP-2 from *Caenorhabditis elegans* is expressed in the sensory neuron pair AWA and contributes to lysosome formation and lipid storage within the intestine. Biochem. Biophys. Res. Commun. *338*, 862–871.

Ohara, T., Ohashi-Kobayashi, A., and Maeda, M. (2008). Biochemical characterization of transporter associated with antigen processing (TAP)-like (ABCB9) expressed in insect cells. Biol. Pharm. Bull. *31*, 1–5.

Ohashi-Kobayashi, A., Ohashi, K., Du, W. B., Omote, H., Nakamoto, R., Al-Shawi, M., and Maeda, M. (2006). Examination of drug resistance activity of human TAP-like (ABCB9) expressed in yeast. Biochem. Biophys. Res. Commun. *343*, 597–601.

Raizen, D. M., Lee, R. Y., and Avery, L. (1995). Interacting genes required for pharyngeal excitation by motor neuron MC in *Caenorhabditis elegans*. Genetics *141*, 1365–1382.

Ruaud, A. F., Nilsson, L., Richard, F., Larsen, M. K., Bessereau, J.-L., and Tuck, S. (2009). The *C. elegans* P4-ATPase TAT-1 regulates lysosome biogenesis and endocytosis. Traffic *10*, 88–100.

Schaheen, L., Patton, G., and Fares, H. (2006). Suppression of the *cup-5* mucolipidosis type IV-related lysosomal dysfunction by the inactivation of an ABC transporter in *C. elegans*. Development *133*, 3939–3948.

Schroeder, L. K., Kremer, S., Kramer, M. J., Currie, E., Kwan, E., Watts, J. L., Lawrenson, A. L., and Hermann, G. J. (2007). Function of the *Caenorhabditis elegans* ABC transporter PGP-2 in the biogenesis of a lysosome-related fat storage organelle. Mol. Biol. Cell *18*, 995–1008.

Sheps, J. A., Ralph, S., Zhao, Z., Baillie, D. L., and Ling, V. (2004). The ABC transporter gene family of *Caenorhabditis elegans* has implications for the evolutionary dynamics of multidrug resistance in eukaryotes. Genome Biol. *5*, R15.

Sundaram, P., Echalier, B., Han, W., Hull, D., and Timmons, L. (2006). ATP-binding cassette transporters are required for efficient RNA interference in *Caenorhabditis elegans*. Mol. Biol. Cell *17*, 3678–3688.

Thomas, J. H. (1990). Genetic analysis of defecation in *Caenorhabditis elegans*. Genetics *124*, 855–872.

Togo, S. H., Maebuchi, M., Yokota, S., Bun-Ya, M., Kawahara, A., and Kamiryo, T. (2000). Immunological detection of alkaline-diaminobenzidine-negative peroxisomes of the nematode *Caenorhabditis elegans* purification and unique pH optima of peroxisomal catalase. Eur. J. Biochem. *267*, 1307–1312.

Uebel, S., Kraas, W., Kienle, S., Wiesmuller, K. H., Jung, G., and Tampe, R. (1997). Recognition principle of the TAP transporter disclosed by combinatorial peptide libraries. Proc. Natl. Acad. Sci. USA *94*, 8976–8981.

Vatamaniuk, O. K., Bucher, E. A., Sundaram, M. V., and Rea, P. A. (2005). CeHMT-1, a putative phytochelatin transporter, is required for cadmium tolerance in *Caenorhabditis elegans*. J. Biol. Chem. *80*, 23684–23690.

Wolters, J. C., Abele, R., and Tampe, R. (2005). Selective and ATP-dependent translocation of peptides by the homodimeric ATP binding cassette transporter TAP-like (ABCB9). J. Biol. Chem. *280*, 23631–23636.

Wu, Y. C., and Horvitz, H. R. (1998). The *C. elegans* cell corpse engulfment gene *ced-7* encodes a protein similar to ABC transporters. Cell *93*, 951–960.

Yabe, T., Suzuki, N., Furukawa, T., Ishihara, T., and Katsura, I. (2005). Multidrug resistance-associated protein MRP-1 regulates dauer diapause by its export activity in *Caenorhabditis elegans*. Development *132*, 3197–3207.

Yamaguchi, Y., Iseoka, H., Kobayashi, A., and Maeda, M. (2004). The carboxyl terminal sequence of rat transporter associated with antigen processing (TAP)-like (ABCB9) is heterogeneous due to splicing of its mRNA. Biol. Pharm. Bull. *27*, 100–104.

Yamaguchi, Y., Kasano, M., Terada, T., Sato, R., and Maeda, M. (1999). An ABC transporter homologous to TAP proteins. FEBS Lett. *457*, 231–236.

Young, L., Leonhard, K., Tatsuta, T., Trowsdale, J., and Langer, T. (2001). Role of the ABC transporter Mdl1 in peptide export from mitochondria. Science *291*, 2135–2138.

Zhang, F., Zhang, W., Liu, L., Fisher, C. L., Hui, D., Childs, S., Dorovini-Zis, K., and Ling, V. (2000). Characterization of ABCB9, an ATP binding cassette protein associated with lysosomes. J. Biol. Chem. *275*, 23287–23294.

Zhao, C., Haase, W., Tampe, R., and Abele, R. (2008). Peptide specificity and lipid activation of the lysosomal transport complex ABCB9 (TAPL). J. Biol. Chem. *283*, 17083–17091.

Zhao, Z., Sheps, J. A., Ling, V., Fang, L. L., and Baillie, D. L. (2004). Expression analysis of ABC transporters reveals differential functions of tandemly duplicated genes in *Caenorhabditis elegans*. J. Mol. Biol. *344*, 409–417.